Defect passivation in multicrystalline silicon for solar cells

I. Tarasov[a] and S. Ostapenko
University of South Florida, 4202 E. Fowler Avenue, Tampa, Florida 33620

K. Nakayashiki and A. Rohatgi
Georgia Institute of Technology, Atlanta, Georgia 30322-0250

(Received 2 July 2004; accepted 7 September 2004)

We report on the effect of hydrogen passivation in ribbon multicrystalline silicon (mc-Si) wafers from SiN_x:H anti-reflecting layer using simultaneous rapid thermal annealing of Al back-contact and SiN_x anti-reflection coating on the front (RTP-Al/SiN_x). Scanning room-temperature photoluminescence spectroscopy revealed a strong inhomogeneity in the increase of minority carrier lifetime caused by the hydrogen defect passivation in mc-Si. We present experimental evidence that RTP-Al/SiN_x processing leads to strong lifetime enhancement caused by hydrogen defect passivation in low-lifetime regions of mc-Si wafers. Additional details on the hydrogenation mechanism are revealed in a course of the dehydrogenation study. Hydrogen out-diffusion shows a different rate or activation energy between high and low lifetime regions of the wafers. © *2004 American Institute of Physics*. [DOI: 10.1063/1.1815380]

Impressive growth in the photovoltaic market over the past decade has been predominantly driven by advances in crystalline silicon technology. Multicrystalline silicon (mc-Si), which is produced by many competing techniques, can meet low-cost production, high solar cell throughput, and high efficiency requirements.[1,2] The importance of the defect passivation or elimination in low-cost mc-Si wafers is recognized as a key requirement for achieving high efficiency solar cells. Solar cell production employs a set of process steps, which realize improvement in the material's quality. These manufacturing steps include (a) phosphorous diffusion, (b) hydrogenation from the amorphous SiN_x:H layer, and (c) Al back-contact firing. It was established recently that combined effect of simultaneous (b)+(c) steps using rapid thermal processing (RTP) technique provides additional benefits to solar cell efficiency through the hydrogen-mediated defect reduction.[3] This hydrogen passivation approach tentatively accounted for increased hydrogen incorporation in defect-enriched regions of mc-Si wafers and solar cells. In this letter, we report on a scanning room-temperature photoluminescence (PL) spectroscopy study of the hydrogen mechanism due to simultaneous rapid thermal annealing of Al on the back and SiN_x on the front (RTP-Al/SiN_x).

For the PL excitation, the 800 nm pulse AlGaAs laser diode with 140 mW peak power was used. The PL mapping setup and procedure are published elsewhere.[4] Materials used in this study were boron doped ~300-μm-thick ribbon mc-Si wafers grown by edge-defined film-fed growth (EFG) method. A set of commercial EFG wafers was prepared and processed as specified in Table I. Each processing step was followed with PL mapping measurement at two principal luminescence bands, as described subsequently.

The PL spectrum of mc-Si wafers at room temperature is composed of two luminescence bands. The first band (I_{BB}) shows a spectral maximum at 1.09 eV and corresponds to band-to-band recombination in silicon. This band was characterized in a broad temperature range up to 750 K and attributed to direct recombination of free and bound to exciton electron–hole pairs.[5] The second "defect" band at 0.8 eV (I_{Def}) is observed only at selected regions on the wafer, and corresponds to deep luminescent defects located around the dislocation lines in mc-Si.[6] This defect band is a fingerprint of the low lifetime regions on wafers and caused by dislocations contaminated by impurity precipitates.[4] PL maps with reasonable spatial resolution can be used to deduce (a) the distribution of the effective minority carrier lifetime (τ_{eff}),[7] (b) the lifetime variation after a solar cell processing, and (c) the maps of the defect centers causing 0.8 eV PL band. The τ_{eff} is composed of radiative, nonradiative, and surface recombinations and, in general, is dominated by nonradiative recombination in Si. In a simple case neglecting diffusion of the photogenerated minority carriers, the I_{BB} and I_{Def} can be expressed as follows.[4]

$$I_{BB} = C_1 \times G \times \tau_{eff}/\tau_{rad}, \tag{1}$$

$$I_{Def} = C_2 \times G \times \tau_{eff}/\tau_{SRH}, \tag{2}$$

where G is the electron–hole pair's photogeneration rate, τ_{rad} is the radiative recombination lifetime, $\tau_{SRH}=(N_{Def}\, v_{th}\, \sigma_n)^{-1}$ is the Shockley–Read–Hall (SRH) radiative lifetime, N_{Def} is the defect concentration, v_{th} and σ_n are the electron thermal velocity and capture cross section, respectively, and C_1 and C_2 are temperature-dependent Si constants. A parameter $R=I_{Def}/I_{BB}$ can be introduced to measure the point-by-point ratio of two PL intensities. Following Eqs. (1) and (2), it is clear that

$$R = I_{Def}/I_{BB} = \text{const} \times N_{Def}; \tag{3}$$

that is, the R parameter allows directly accessing the PL defect concentration and their spatial distribution with the PL mapping procedure. Notice that the R value is independent on other recombination defects in the bulk and at the surface, which contribute to τ_{eff}.

Figures 1(a) and 1(b) show two PL maps, I_{BB} and I_{Def}, respectively, collected at identical points on the same 50 mm × 22 mm EFG wafer after the 750 °C RTP-Al/SiN_x hydrogenation step. The distribution of I_{BB} maintains a pro-

[a]Electronic mail: itarasov@eng.usf.edu

TABLE I. Flowchart of processing steps and PL results in EFG wafers. Average across the wafer values of the band-to-band PL (I_{BB}), defect band PL (I_{Def}), and R parameter ($R=I_{Def}/I_{BB}$) on sample #2 before and after each processing step are summarized.

Step	Sample stage	Processing	I_{BB}	I_{Def}	R
1	Initial		28.8	[a]	[a]
2	Hydrogenation	SiN_x deposition, Al back-contact screen-print, RTP annealing at 750 °C for 1 s, and removing SiN_x layer in 50% HF solution.	126.3	0.71	0.011
3	Dehydrogenation (600 °C)	RTP annealing at 600 °C for 1 s in N_2/O_2 ambient	112.5	0.61	0.013
4	Dehydrogenation (700 °C)	RTP annealing at 700 °C for 1 s in N_2/O_2 ambient	42.8	0.34	0.024

[a]Defect band intensity is below sensitivity limit of the PL system.

file of the effective lifetime according to Eq. (1) as published in Ref. 4. The areas with low I_{BB} intensity correspond to high recombination activity of *all* defects (low lifetime regions), while the high I_{BB} values represent "good" or high lifetime regions. It was established previously that low I_{BB} regions are specified also by intense I_{Def} band, while in high I_{BB} regions this band is negligible.[4] This reverse contrast of I_{BB} and I_{Def} is illustrated in Figs. 1(a) and 1(b) after the hydrogenation was completed.

Hydrogenation leads to a significant increase in the band-to-band PL intensity (28.8 to 126.3) averaged across the sample, as presented in Table I (wafer #2). This effect can be interpreted as lifetime upgrade due to RTP-Al/SiN_x processing.[8] In different samples, we observed a 1.5–4.3 times hydrogenation-induced increase in average I_{BB} values. Notice that the defect band, which at the initial stage had an intensity below the PL system detection limit, also increased in intensity after the hydrogenation due to the same lifetime upgrade according to Eq. (2). We observe that high PL and low PL areas on EFG wafers respond differently to the RTP-Al/SiN_x processing. Specifically, high PL areas prior to the hydrogenation show quite small, up to 30%, lifetime upgrade effect. In contrast, low PL areas show a spectacular lifetime upgrade, up to *two orders* of magnitude, after the hydrogenation. Evidently, the average across the sample values of I_{BB} increase (Table I) caused by hydrogenation represents a superposition of both areas. To illustrate the lifetime upgrade effect over the wafer one can introduce the upgrade coefficient as the point-by-point ratio of two band-to-band PL intensities, before and after the hydrogenation, as

$$K_{up} = I_{BB}(\text{hydrogenated})/I_{BB}(\text{initial}) = \tau_{eff}(\text{hydrogenated})/\tau_{eff}(\text{initial}). \quad (4)$$

The K_{up} map on the wafer #2 is plotted in Fig. 1(c). To further quantify the lifetime upgrade, we show, in Fig. 2, PL data analyzed on two different areas on sample #2 with (a) low and (b) high band-to-band PL. Consistent with entire mapping in Fig. 1, the low band-to-band PL area (a) shows an average 20-fold lifetime increase, while high band-to-band PL area (b) shows only a 10% upgrade in lifetime. Notice that the y axis on Fig. 2 has a logarithmic scale.

Based on our study, we conclude that RTP-Al/SiN_x hydrogenation significantly improves "bad" regions in EFG wafers, and has little effect on the high lifetime areas.

To further explore the hydrogen incorporation mechanism in mc-Si, we performed two consecutive RTP annealings at 600 and 700 °C on the previously hydrogenated wafers after etching off the SiN_x:H layer (see Table I for the

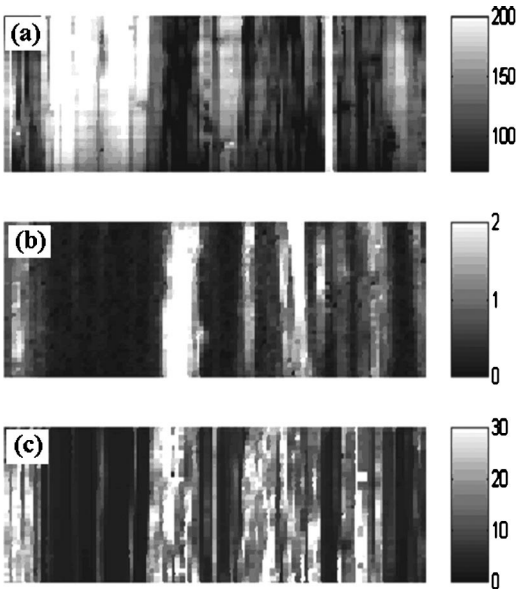

FIG. 1. Room-temperature PL mapping (a) band-to-band PL, (b) defect band PL, and (c) point-by-point ratio of I_{BB}(hydrogenated)/I_{BB}(initial) representing lifetime upgrade effect. The mapping size is 50 mm × 22 mm, step = 0.5 mm.

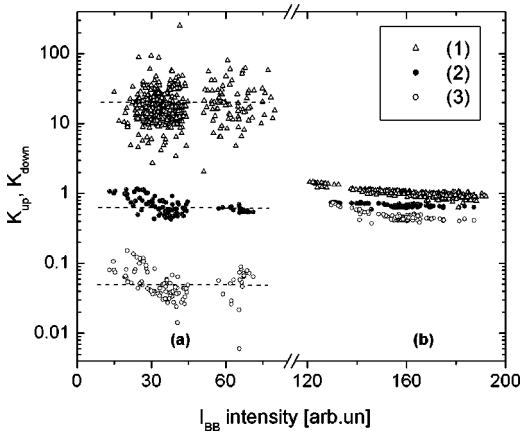

FIG. 2. Lifetime upgrade and downgrade coefficients measured in areas with (a) low and (b) high band-to-band PL intensity. (1) Corresponds to RTP-Al hydrogenation, (2) 600 °C RTP dehydrogenation, and (3) 700 °C RTP dehydrogenation.

processing details). It was demonstrated recently that the average effective lifetime decreased after this processing step due to hydrogen out-diffusion, and reduction of bulk lifetime can lead to significant loss in solar cell efficiency.[3] In Table I, we show PL results of such a dehydrogenation experiment on wafer #2. Consistent with the lifetime data in literature, the RTP at 600 and 700 °C led to a gradual decrease in the PL intensity of both the luminescent bands, this is consistent with the hydrogen out-diffusion model for the observed lifetime downgrade.[8]

Similar to the hydrogenation case, we analyzed the I_{BB} variation across the wafers after each dehydrogenation anneal step. We calculated at every mapped spot the ratio of the band-to-band PL intensities after the RTP with respect to the hydrogenated stage by introducing the downgrade coefficient

$$K_{\text{down}} = I_{BB}(\text{dehydrogenated})/I_{BB}(\text{hydrogenated}) = \tau_{\text{eff}}(\text{dehydrogenated})/\tau_{\text{eff}}(\text{hydrogenated}). \quad (5)$$

In Fig. 2, the K_{down} data points are shown for the same wafer regions as in the hydrogenation experiment, allowing comparing them with K_{up} distributions. In addition to the PL degradation across the entire sample, two other effects were observed. First, the low PL intensity region "a" showed much stronger lifetime downgrade than high PL region "b." Specifically, we observed up to 50-fold decrease in the PL intensity in the area "a" versus only a factor of 2 decrease in the area "b." Secondly, the PL intensity degradation due to RTP dehydrogenation annealing showed a different temperature annealing rate in "a" compared to "b" regions. This is evident by comparing points labeled as (2) and (3) in both areas representing 600 and 700 °C anneal steps, correspondingly. The rate of temperature annealing is directly proportional to the activation energy of the hydrogen out-diffusion process. Having this in mind, we conclude that the activation energies are quite different in both regions; lower in the low lifetime regions and higher in the high lifetime regions. Moreover, the rapid decrease in I_{BB} in area "a" is consistent with the reported lifetime degradation.[8]

To elaborate on details of the hydrogenation and dehydrogenation processes, we present, in Fig. 3, three PL line scans measured and calculated at identical wafer location. Data (a) represent the line scan for the downgrade coefficient after the 700 °C RTP dehydrogenation anneal. Notice that K_{down} shows up to a 10 times reduction in lifetime in the areas marked by arrows. Data points in Fig. 3(b) represent the R parameter calculated according to Eq. (3) after the hydrogenation (open circles) and subsequent dehydrogenation (closed circles) at 700 °C. First, notice that a clear inverse correlation between K_{down} and R parameter or the defect concentrations. Secondly, comparison of R parameter distribution after the RTP-Al/SiN_x hydrogenation and subsequent 700 °C dehydrogenation reveals that the increase in the R parameter or the PL defect concentration is caused by hydrogen out-diffusion. This line-scan experiment is statistically in agreement with the behavior over the entire EFG wafer area, as illustrated in Table I.

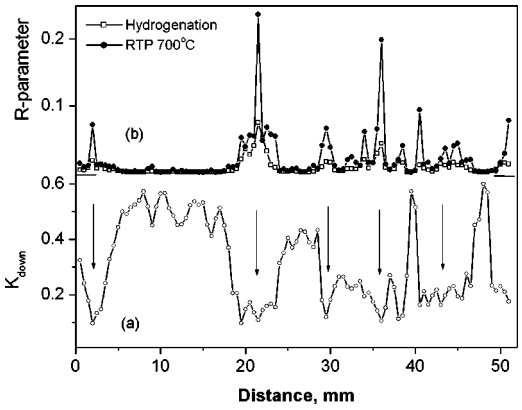

FIG. 3. Lines scans of (a) downgrade coefficient after dehydrogenation cased by 700 °C RTP, and (b) R parameter after RTP-Al hydrogenation (open circles) and after 700 °C dehydrogenation (closed circles). Spatial match of strongest downgrade lifetime effect and R-parameter peaks indicated by arrows.

In conclusion, scanning spectroscopic PL experiments on hydrogenated and dehydrogenated EFG mc-Si wafers identified that the major effect of the RTP-Al/SiN_x anneal process consists of hydrogen incorporation into the regions with high recombination activity of defects involving contaminated dislocations. Hydrogenation passivates radiative and nonradiative dislocation defects in the low lifetime regions, improving the local minority carrier lifetime, which benefits the solar cell efficiency.

The authors would like to thank B. R. Bathey at RWE Schott Solar, Inc. for material supply. The work was supported in part by NREL subcontracts ACQ-9-29639-03 and ATT-2-31605-02 and U.S. DOE subcontract DE-FC36-00GO10600.

[1] S. Narasimha and A. Rohatgi, IEEE Trans. Electron Devices **45**, 1776 (1998).
[2] A. Rohatgi, D. S. Kim, K. Nakayashiki, V. Yelundur, and B. Rounsaville, Appl. Phys. Lett. **84**, 145 (2004).
[3] V. Yelundur, A. Rohatgi, A. Ebong, A. M. Gabor, J. I. Hanoka, and R. L. Wallace, J. Electron. Mater. **30**, 526 (2001).
[4] S. Ostapenko, I. Tarasov, J. P. Kalejs, C. Haessler, and E.-U. Reisner, Semicond. Sci. Technol. **15**, 840 (2000).
[5] V. Alex, S. Finkbeiner, and J. Weber, J. Appl. Phys. **79**, 6943 (1996).
[6] S. Ostapenko and M. Romero, Eur. Phys. J.: Appl. Phys. (in press).
[7] I. Tarasov, S. Ostapenko, V. Feifer, S. McHugo, S. V. Koveshnikov, J. Weber, C. Haessler, and E.-U. Reisner, Physica B **273–274**, 549 (1999).
[8] K. Nakayashiki, D. S. Kim, A. Rohatgi, B. R. Bathey, Technical Digest of 14th International Photovoltaics Science and Engineering Conference, Bangkok, Thailand, 2004, p. 643.